https://doi.org/10.5194/hess-2020-190
Preprint. Discussion started: 26 May 2020
© Author(s) 2020. CC BY 4.0 License.

Hydrology and Earth System Sciences
Discussions

Long-term water stress and drought monitoring of Mediterranean oak savanna vegetation using thermal remote sensing

María P. González-Dugo[1*], Xuelong Chen[2,3], Ana Andreu[1], Elisabet Carpintero[1], Pedro J. Gómez-Giraldez[1], Arnaud Carrara[4], Zhongbo Su[5]

[1]IFAPA, Consejería de Agricultura, Pesca y Desarrollo Rural. Apdo. 3048 ES-14071 Cordoba, Spain

[2] Key Laboratory of Tibetan Environment Changes and Land Surface Processes, Institute of Tibetan Plateau Research, Chinese Academy of Sciences, Beijing, China

[3] CAS Center for Excellence in Tibetan Plateau Earth Sciences, Chinese Academy of Sciences, Beijing, China

[4] Fundación CEAM. Parque Tecnológico,14 Calle Charles Darwin. Paterna (Valencia), Spain 46980

[5]Faculty of Geo-Information Science and Earth Observation, University of Twente, Enschede, the Netherlands

Correspondence to: María P. González-Dugo (mariap.gonzalez.d@juntadeandalucia.es)

Abstract. Drought is a devastating natural hazard, difficult to define, detect and quantify. Global meteorological data and remote sensing products present new opportunities to characterize drought in an objective way, and to extend this analysis in space and time. In this paper, we applied the surface energy balance model SEBS (Surface Energy Balance System) for the period 2001-2018, to estimate evapotranspiration and other energy fluxes over the *dehesa* area of the Iberian Peninsula, with a monthly temporal resolution and 0.05º pixel size. A satisfactory agreement was found between the fluxes modelled and the measurements obtained for three years by two flux towers located over representative sites (RMSD= 21 W m^{-2} and R^2 of 0.76, for all energy fluxes and both sites). The estimations of the convective fluxes (LE and H) showed higher deviations, with RMSD = 26 W m^{-2} on average, than Rn and G, with RMSD = 15 W m^{-2}. At both sites, annual ET was very close to total precipitation with the exception of a few wet years in which intense precipitation events, producing high run-off, were observed. The analysis of the anomalies of the ratio of evapotranspiration (ET) to reference ET (ET_o) was used as an indicator of agricultural drought on monthly and annual scales. Hydrological years 2004/2005 and 2011/2012 stood out for their negative values, with the first one being the severest of the series, the impact observed on vegetation coverage and grain production. On a monthly scale, this event was also the longest and most intense, with peak negative values in January-February and April-May of 2005, explaining its great impact on cereal production (up to 45% reduction). During the drier events, the changes in vegetation ground cover over the months, with a preponderant presence of grasslands compared with those in which only oak trees were active, allowed a separate analysis of the strategies adopted by the two strata to cope with water stress. These results indicate that the drought events characterized for the period did not cause any permanent damage

https://doi.org/10.5194/hess-2020-190
Preprint. Discussion started: 26 May 2020
© Author(s) 2020. CC BY 4.0 License.

Hydrology and Earth System Sciences
Discussions

on the vegetation of *dehesa* systems. The approach tested has proved useful to provide insight into the characteristics of drought events over this ecosystem and will be helpful to identify areas of interest for future studies at finer resolutions.

1 Introduction

Drought is a devastating natural hazard, globally widespread, and with complex consequences across spatio-temporal scales and sectors. Unlike other disasters, it is still a challenge to define, detect and quantify droughts (Sheffield and Wood, 2011), impeding most prevention and mitigation actions. When droughts affect savannas, the two canopies of this ecosystem, grasslands and trees/shrubs, suffer from different stresses: (i) the pasture production is reduced or lost, with a direct economic consequence resulting from the need to supplement animal feeding and, in more severe situations, the death or premature sale of animals; (ii) the decline and dieback of trees affect the ecosystem structure, jeopardizing the long-term conservation of the system (Fenshan and Holman, 1999). Traditional agropastoral systems in arid and semiarid areas have developed strategies to cope with drought, such as diversifying into crops and livestock, into animal species and breeds, or fluctuating herd sizes (Hazell et al., 2001). More recently, insurance services for damage caused by water stress to pasture production provide farmers with a means for recovery after a disaster. However, the slow-onset nature of drought, the large extension of savanna areas and their complex canopy structure pose additional difficulties to the already challenging monitoring of drought and its damage assessment.

The increasing availability of global meteorological data and new remote sensing products, with advanced processing services and free and open data, offers an opportunity to characterize drought objectively, and to extend its analysis in space and time. Many indicators using remote-sensing inputs have been developed in the last decades (Wardlow et al., 2012). Surface energy balance models (SEBM) provide a physically based rationale to combine the most often used remote-sensing retrievals for drought monitoring: vegetation indices (VIs) and land surface temperature (LST). The VIs provide information about the amount and condition of the vegetation (Jackson and Huete, 1991), while the land surface temperature describes the state of the surface and the partitioning of the available energy into sensible heat (H) and latent heat (LE) or evapotranspiration (ET) (Kustas and Norman, 1996). LST and VIs combined in SEBMs have provided accurate estimations of ET over agriculture (Anderson et al., 2015; Allen et al., 2011; Cammalleri et al., 2012; Andreu et al., 2015; Gonzalez-Dugo et al., 2009, 2012) and agroforestry systems (Andreu, 2018a,b; Guzinski et al. 2018; Carpintero et al. 2016). The evapotranspiration of a canopy is a suitable indicator of its water status and a good measurement of the impact of water shortage on vegetation and on the ecosystem functioning. Evapotranspiration and soil moisture anomalies have been widely used for spatially distributed monitoring of agricultural drought (Anderson et al., 2016; Cammalleri el al., 2015; Sheffield et al., 2004). These anomalies underline the abnormally dry conditions when compared to the usual state of an ecosystem, derived from historical data. Evapotranspiration anomalies were used here to monitor drought and vegetation water stress over the holm oak savanna area of the Iberian Peninsula during a period of seventeen years.

https://doi.org/10.5194/hess-2020-190
Preprint. Discussion started: 26 May 2020
© Author(s) 2020. CC BY 4.0 License.

Hydrology and Earth System Sciences
Discussions

The Mediterranean oak savanna, called *dehesa* in Spain and *montado* in Portugal, is the most extensive and representative agroforestry system in Europe, with more than 3 million hectares in the Iberian Peninsula (Moreno and Pulido, 2009). It is a man-made ecosystem that maintains a fragile balance between its multiple uses (livestock, cereal crops, cork, hunting, etc.) and the conservation of its natural resources. The *dehesa's* diversity of habitats, giving refuge to a large number of species (Díaz et al., 1997), is especially recognized, and it is listed as having community-wide interest in the EU habitat directive (92/43/EEC). It is a water-controlled system, with its productivity directly dependent on water availability. Mediterranean oaks have the ability to dampen the effects of water scarcity through a complex combination of drought resistance mechanisms with different time scales, as shown by Rambal (1993) for *Quercus coccifera L.* However, an additional problem to the recurrent water scarcity, is the identification of low soil water content as an initiating factor involved in the severe oak decline affecting a large area of *dehesa* since the early 1980s (Sánchez et al., 2002). Drought events impede the growth of *Q. ilex* seedlings and increase their susceptibility to *Phytophthora cinnamomic* (Corcobado et al., 2014), the main biotic factor responsible for this decline (Sánchez et al., 2002).

In this work, a surface energy balance model, SEBS (Surface Energy Balance System) (Chen et al., 2013, Su, 2002) has been applied to estimate evapotranspiration and other energy fluxes from 2001 to 2018 over the *dehesa* areas of Spain and Portugal. A first objective was to validate the energy fluxes produced by this model over the *dehesa* landscape. The second was to analyze the anomalies of the ratio of ET to reference ET as an indicator of agricultural drought in this environment at monthly and annual scales and use it to characterize the main drought events occurring in this period in space and time.

2 Data and methodology

The study was conducted over the oak savanna area of the Iberian Peninsula (Figure 1) using data from January 2001 to August 2018. This ecosystem covered 3.12 million ha in 2006 according to the European CORINE Land Cover inventory (CLC2006. 100 m - version 12/2009 https://www.eea.europa.eu/data-and-maps/data/ clc-2006-raster-4). The area has remained fairly stable during the study period, with changes of less than 1.5% between CLC2006 and the previous and posterior inventories, in 2000 and 2012.

2.1 SEBS model description and application

A revised version of the surface energy balance system model known as SEBS (Su, 2002; Chen et al., 2013) was used to estimate land heat fluxes integrating remote sensing and meteorological forcing data. The new parameterization of the bare soil excess resistance to heat transfer, included in the revised version, improved the model's performance especially for bare soil and low canopy surfaces (Chen et al., 2013). The latent heat flux (LE) was computed as a residual of the surface energy balance equation:

$$Rn = \mathrm{G} + \mathrm{H} + \mathrm{LE}\,, \quad (1)$$

https://doi.org/10.5194/hess-2020-190
Preprint. Discussion started: 26 May 2020
© Author(s) 2020. CC BY 4.0 License.

Hydrology and Earth System Sciences
Discussions

where Rn is the net radiation, G is the soil heat flux and H is the turbulent sensible heat flux. The net radiation is calculated with the following equation:

$$R_n = (1-\alpha)SW_d + \varepsilon LW_d - \varepsilon\sigma LST^4 \quad (2)$$

Where α is broadband albedo; SW_d is the downward short-wave radiation; LW_d, the downward long-wave radiation; ε, the land surface emissivity; σ, the Stefan-Bolzmann constant; and LST, the land surface temperature.

The soil heat flux is derived from its ratio to the net radiation (Γ) using equation 3:

$$G = R_n[\Gamma_C + (1-f_C)(\Gamma_S - \Gamma_C)] \quad (3)$$

This ratio is assumed to be equal to 0.05 (Monteith, 1973) for surfaces with fully covered vegetation (Γ_C) and 0.315 for bare soils (Γ_S) (Kustas and Daughtry, 1990). The green canopy cover, f_c, is determined using the normalized difference vegetation index (NDVI) in equation 8.

Using equations 1 to 3 and energy balance considerations at limiting cases, the following reductions can be applied: (i) under the dry limit (equations 4 and 5), the evapotranspiration is assumed to become zero, λE_{dry} and the sensible heat flux is at its maximum, H_{dry}.

$$\lambda E_{dry} = R_n - G \quad - H_{dry} \equiv 0 \quad (4)$$

$$H_{dry} = R_n - G \quad (5)$$

(ii) under the wet limit (equations 6 and 7), the evaporation is only limited by the available energy at the given surface and atmospheric conditions, λE_{wet}, and the sensible heat takes its minimum value H_{wet}:

$$\lambda E_{wet} = R_n - G \quad - H_{wet} \quad (6)$$

$$H_{wet} = R_n - G \quad - \lambda E_{wet} \quad (7)$$

The sensible heat is computed according to the Monin-Obukhov similarity theory and limited by the dry and wet conditions. H_{dry} is given by equation 5 and H_{wet} is derived using equation 7 and the application of a set of assumptions for extremely wet conditions to the Penman-Monteith equation (Menenti, 1984). A complete description of the model can be found in Su (2002).

The parametrization of two surface variables, f_c and the height of the canopy (h_c), has been adapted to the specific characteristics of *dehesa* ecosystems. The green canopy cover and leaf area index (L) were calculated using the following equations (Choudhury et al., 1994):

$$(1-f_c)^{\xi} = \frac{NDVI_{max} - NDVI}{NDVI_{max} - NDVI_{min}} \quad (8)$$

$$f_c = 1 - \exp(-kL) \quad (9)$$

https://doi.org/10.5194/hess-2020-190
Preprint. Discussion started: 26 May 2020
© Author(s) 2020. CC BY 4.0 License.

Hydrology and Earth System Sciences
Discussions

where $NDVI_{max}$ and $NDVI_{min,}$ represent a surface fully covered by vegetation (~0.94) and completely bare (~0.15), respectively. The parameter ξ represents the ratio of the canopy extinction coefficient (*K'*) to a leaf angle distribution term (*k*). *k* was assumed to be equal to 0.5 for a random distribution of leaves, as the ecosystem contains erectophile grasses and planophile oak tree leaves (Andreu et al., 2019). *K'* adopted a value of 0.8 obtained from experimental data and within the range proposed for NDVI by Baret and Guyot (1991).

The height of the canopy was computed to account for variations in the tree component, with a greater influence on the average height of the system than short and more variable pasture. An annual value of canopy h_c was estimated for every pixel during the summer, when oaks are the only green vegetation contributing to the pixel spectral response. An effective value of h_c for the year was estimated based on the tree coverage, assessed using the summer value of the NDVI, and an average tree height of 8 m, representative of the predominant tree species *Quercus ilex sp*.

The model was applied over the entire Iberian Peninsula using monthly data with a spatial resolution of 0.05°. Satellite and meteorological data sources are described in Table 1. Albedo, land surface temperature (LST), surface emissivity and leaf area index (LAI) were derived from different products of MODIS sensor. Meteorological data were provided by the ERA-Interim, a global atmospheric reanalysis data set from the European Centre for Medium-range Weather Forecast.

To analyze model results, the monthly rainfall gridded data of the Climatic Research Unit (CRU) Time-Series (TS) Version 3.21 (Harris et al., 2014), provided by the Global Climate Monitor System (Camarillo-Naranjo et al., 2019), have been averaged over the *dehesa* area of the Iberian Peninsula.

2.2 Validation sites

Two experimental sites (Figure 1) with similar flux measurement instrumentation have been used to validate the evapotranspiration and other energy fluxes estimated using the SEBS model. Detailed information on the measurements and the processing of the data can be found in Andreu et al. (2018a and b). Both eddy covariance towers, named Sta.Clo (Santa Clotilde, Andalusia, 38°12′N; 4°17′W, 736 m a.s.l.) and ES-LMa (Boyal de Majadas del Tiétar, Extremadura, 39°56′N; 5°46′W, 260 m a.s.l.) are located over *dehesa*-type ecosystems under similar management and a landscape of scattered oak trees with a fractional cover of around 20%, in southern and southwestern Spain, respectively. The convective fluxes of the systems are measured above the tree height (at 17 m in Sta.Clo and 15 m in ES-LMa) with closure balance errors of 20% and 14%, both values being within the range found by other authors (Foken, 2008; Franssen et al., 2010). Soil moisture, precipitation and other complementary measurements of the vegetation (reflectance, LAI, green canopy cover) were used to characterize the dynamics of the vegetation and the soil water status throughout the year.

The area contributing most to the fluxes measured was estimated by using Schuepp et al. (1990) and varied between 1 and 2 km. These footprints are lower than the pixel size of 5 km used for the application of the SEBS model. However, the homogeneity of the system, with similar tree ground cover fraction and pasture management at several kilometers around the

https://doi.org/10.5194/hess-2020-190
Preprint. Discussion started: 26 May 2020
© Author(s) 2020. CC BY 4.0 License.

Hydrology and Earth System Sciences
Discussions

towers supported the capacity of these sites to serve as a reference for the validation of modelled fluxes. Also verified in both cases was the good correspondence between the model input meteorological data at the tower's location and the ground measurements (data not shown).

Monthly rainfall data for the seventeen years of the study was provided by the closest weather station to each site, located at 3 km and 16 km of Sta.Clo and ES-LMa towers, respectively. Both of them are operated by the Spanish Meteorology Agency (AEMET).

2.3 Water stress calculations

The relative evapotranspiration is the ratio of actual to potential or reference ET (ET/ET_o). It has been used as an indicator of crop water stress (Anderson et al., 2015, 2016), of drought (Anderson et al., 2011), and as a proxy for soil moisture (Su et al., 2003). The same approach is used worldwide in irrigation engineering to compute crop water requirements following FAO (24 and 56) guidelines (Doorenbos and Pruitt, 1977; Allen et al, 1998).

Anomalous water stress conditions indicating drought were assessed here with the standardized values of relative ET. FAO56 reference ET (Allen et al., 1998) was selected to estimate the atmospheric evaporative demand (AED), given the difficulties of reproducing the biological control of the transpiration, even at potential rates, of the different types of vegetation conforming this ecosystem.

The vegetation water stress caused by the long dry summers of the Mediterranean climate can be considered to be the 'normal' state of the system for several months of the year. To identify unusually dry conditions indicating drought, standard (z) scores of this variable (ET/ET_o) for a given month/year have been computed. This standardization procedure assumes that the data follow a normal distribution. Some authors (Sheffield et al., 2004; Cammalleri et al., 2015) have pointed out that soil moisture and the water deficit index derived from it are generally characterized by a skewed distribution and can be statistically better represented using the beta distribution. In this case, the analysis of the ET and relative ET time series indicated that even when the histograms of both time series followed a skewed distribution, more pronounced in the case of the actual than the relative ET, the values of mean, median and mode of the relative ET series were very similar, backing up the use of z scores for the standardization of this variable.

Two variables, vegetation coverage (f_c) and rain-fed wheat production, have been selected as drought impact indicators. Winter cereals are the main cropping system of these areas, in which the low fertility of the soils does not allow a more intense agricultural use. Annual yield statistics (http://www.mapama.gob.es/es/estadistica/temas/estadisticas-agrarias/agricultura/esyrce/) have been gathered and aggregated for the *dehesa* area (Figure 1).

https://doi.org/10.5194/hess-2020-190
Preprint. Discussion started: 26 May 2020
© Author(s) 2020. CC BY 4.0 License.

Hydrology and Earth System Sciences
Discussions

3 Results and discussion

3.1 Model validation

The comparison of SEBS model estimation of monthly energy fluxes with measurements at the two EC towers during a total of six years, 2009 to 2011 for ES-LMa and 2015 to 2017 for Sta.Clo, displayed in Figure 2, presented a general good agreement, with an average root mean square difference (RMSD) of 21 W m^{-2} and R^2 of 0.76, for all energy fluxes and both sites. The estimations of the convective fluxes (LE and H) show higher deviations, with RMSD =26W m^{-2} on average, than Rn and G, with RMSD = 15 W m^{-2}. Model performance at ES-LMa site was, in general, superior to that at Sta.Clo, with all the statistics metrics computed for the comparison (RMSD, MBE and R^2) presenting lesser dispersion and slightly lower errors. LE was slightly overestimated at both sites (MBE =10.3 and 2.8 W m^{-2} at Sta.Clo and ES-LMa, respectively), which is in agreement with previous applications of the model (Michel et al., 2016). This overestimation was particularly significant for some springtime months at Sta.Clo, when the sensible heat was underestimated by the SEBS model (Chen et al., 2019). However, LE estimations presented a similar or lower RMSD than other applications of the SEBS model (Chen et al. 2014; Vinukollu et al, 2011). In particular, the work by Chen et al. (2014) estimated energy fluxes over China at the same temporal scale and with similar input databases. The comparison with measurements at 11 Chinese flux towers presented results that were very close to the ones obtained by this application. Mean RMSDs for all fluxes were alike (RMSD = 22 W m^{-2} was reported by Chen et al. (2014)), with a marginally better performance for convective fluxes and a poorer one for Rn and G (RMSDs in China were 22 and 24 W m^{-2} for convective fluxes and, Rn and G, respectively).

Figure 3 presents the evolution of modelled ET and ET_o, ET/ET_o and measured precipitation from 2001 to 2018, aggregating the hydrological year (between October 1st and September 30th) at the two experimental sites. It can be observed that annual ET variations for the period followed a similar pattern of precipitation at both sites, confirming the predominant control of water availability over the evaporation in these systems. This control is consequently extended to ecosystem productivity and in most years the water consumption, coupled to biomass production, is close to the total rainfall. Tree density is similar at both sites and the differences in water consumption between them are explained by variations in annual pasture production, due to differences in water availability and soil properties. A few of the years are outside this pattern relating rainfall and ET; this corresponded either to very wet ones, or to years of average rainfall but with the occurrence of intense precipitation events that produced an increase in run-off. This can be observed by the run-off recorded at Sta.Clo watershed reservoir (Figure 3a). The main land-use of this small watershed (48.4 km^2) is *dehesa*, but other uses can be found as well, such as olive groves and field crops. Very low runoff values are recorded in regular and dry years, with peaks for the wet ones.

Annual run-off measurements followed a close relationship (data not shown) with the annual aridity index (Budyko, 1974) estimated at Sta.Clo. On average, we found aridity indices of above one at both sites, indicating dry regions where the evaporative demand cannot be met by precipitation. In this case, AED was computed using Penman-Monteith for comparison purposes. Sta.Clo site is noticeably less arid than ES-LMa, with an aridity index equal to 2.9 and 3.75 on

https://doi.org/10.5194/hess-2020-190
Preprint. Discussion started: 26 May 2020
© Author(s) 2020. CC BY 4.0 License.

Hydrology and Earth System Sciences
Discussions

average for the 17 hydrological years at Sta.Clo and ES-LMa, respectively, with both of them falling under the category of a semi-arid climate regime (Ponce et al., 2000). The two sites presented similar annual ET_o values for the period (Figure 4), but annual precipitation was around 200 mm higher, on average, at Sta.Clo, with a higher and more variable ET/ET_o throughout the years. What can also be observed in Figure 3 is the complementary relationship between actual and reference evapotranspiration at this temporal scale, with the sum of annual ET and ET_o approaching a constant value at both sites, confirming previous hypotheses (Bouchet, 1963; Morton, 1975; Brutsaert and Stricker, 1979).

3.2 Annual drought monitoring and impact assessment

Drought was characterized on an annual scale over the experimental sites and the whole area of the *dehesa* of the Iberian Peninsula using the relative evaporation anomalies. Figure 4 presents their evolution for the two sites throughout the study period. A clear similarity can be observed in the main negative anomalies, which identify the most severe droughts during the years 2004/05 and 2011/12 at both sites, despite the differences in aridity and the distance (Figure 1) between them, indicating the extended area and intensity of both events. Differences are more evident in the case of the mild droughts, occurring at both sites but with different intensities during two periods, 2007 to 2009 and 2016 to 2018.

When the whole *dehesa* area is considered (Figures 5 and 6), a more complete view of the general intensity, impact, and spatial distribution of those dry periods, can be obtained. Figure 5 aggregates for the total *dehesa* area the evolution of the relative ET anomalies, together with variables related to the exchanges of energy between the surface and the atmosphere, the green canopy cover, and the production of rainfed wheat, the last two selected as indicators of the impact of water scarcity on the system.

The two severely dry years identified at the experimental sites were the driest ones for the entire *dehesa* area, with 2004/2005 standing out as the most severe event of the time series. None of them lasted more than one year. For these two dry years, a reduction in the latent heat can be observed when compared to the complete series, producing a swap with the sensible heat in the second position in magnitude of the energy balance components. A rise in the surface temperature, increasing the difference with the air temperature, is also observed for those dry years. The order of severity in dryness, established by the magnitude of negative values of ET/ET_o anomalies, is also observed in their impacts over the system (Figure 6). In 2004/05, the wheat production in the area was reduced by almost half of the average (45%) for the period analysed, and the vegetation groundcover fraction fell by 20% compared to the average of the same period. This severe drought affected the entire Iberian Peninsula, with the Spanish and Portuguese cereal and hydroelectricity productions decreasing by 40% and 60% with respect to the average (Garcia-Herrera et al., 2007) and a 10% reduction in total EU cereal yields (UNEP, 2006). The event during 2011/2012 was among the largest and most severe ones in Europe for the 18-year simulation period analysed by Cammalleri et al. (2015), contributing to a global decline in grain production.

Figure 6 shows maps of ET/ET_o anomalies in Iberia for the seventeen years of the study, highlighting the *dehesa* area of interest in this work. The spatial variability of these anomalies for most years is significant, although prevalently dry and wet

https://doi.org/10.5194/hess-2020-190
Preprint. Discussion started: 26 May 2020
© Author(s) 2020. CC BY 4.0 License.

Hydrology and Earth System Sciences
Discussions

years can be distinguished. In 2004/05 and 2011/12, the drought was severe and affected most of the area of interest, as the aggregated values of Figure 5 also point out. In 2008/09, the water stress was milder in the western area, as can be observed in Figure 6, as at the experimental site of Sta.Clo (Figure 4) located in this part of the region. The recovery of the vegetation water status was generally achieved the year following the dry one in most areas.

3.3 Monthly drought analysis

The monthly evolution of relative evapotranspiration anomalies is displayed in Figure 7a, with negative values indicating water stress conditions highlighted in red. Absolute ET and ET_o values, used to calculate these anomalies, are shown in Figure 7b together with monthly rainfall for the period. One can observe the alternation of complementary and parallel characteristics of ET and ET_o throughout the year, with the longest complementary period indicating water-limited ET conditions starting in May for most of the years, confirmed by the decreasing trend in rainfall starting in that month. At the end of the summer when the first rains arrive the trend of ET and ET_o changes, producing a secondary peak in ET that lasts until the energy-limited parallel phase starts in November. Both variables follow a concurrent rise from January until the soil water deficit limits ET again.

The annual fluctuations of the green canopy cover (thick green line in Figure 7a) followed the expected seasonality of Mediterranean vegetation, corresponding to the dynamics of ET and ET_o changes. The maximum coverage (March and April) corresponds to the peak of grassland production (and ET although with different shape) and the minimum appears during the dry summer, only endured by the oak trees. In some years, the growing season presents a bimodal shape, with an initial peak produced by autumn pastures, which is also reflected in ET values. It can be observed mostly in wet years (e.g. 2003, 2007, 2011), with the vegetation growth following a pattern that can be related to the soil water availability, represented here by the ET/ET_o anomalies.

The duration, in number of months with negative anomalies, and the intensity of each drought event can be quantified, which may help to explain the response of the vegetation during these periods. In this sense, the two main drought events identified on an annual scale (2004/05 and 2011/12), presented dryer than normal conditions during the whole or most of the year. The first event was longer (sixteen months in the first case, prolonging the drought to the beginning of the following year) and with higher negative values than the second one, of an eleven-months duration, explaining the greater impacts detected on the vegetation and cereal yield. Other dry periods, in 2009, 2017 and 2018, presented consecutive negative anomalies for ten to eleven months but, in some cases, the non-homogeneous distribution of the drought observed in Figure 6, may have undermined the impact analysis on this aggregated spatial scale. In terms of impact assessment, the time of the year with peak negative anomalies is important, with springtime events producing greater impacts (e.g. in 2004/2005 the highest negative values corresponded to January, February, April and May of 2005).

During the dry years, the annual vegetation growth pattern varies with respect to the typical one, depending on the duration and severity of drought events. The dynamics of the vegetation in this system allows for a separate analysis of the effect of

https://doi.org/10.5194/hess-2020-190
Preprint. Discussion started: 26 May 2020
© Author(s) 2020. CC BY 4.0 License.

Hydrology and Earth System Sciences
Discussions

water scarcity over trees and pastures. The dashed green lines (Figure 7a) show the changes in annual maximum and minimum values of f_c, with the maximum ones mostly expressing the impact on pasture, and the changes in the minimum ones represent only the impact over the tree canopy. The decreases in pasture f_c are more pronounced than changes in oaks f_c, as grasslands are more abundant, and their roots are mostly located in the first centimetres of soil. On the contrary, the rooting system of the oak tree is in fact adapted to the regular dry periods of the Mediterranean climate, exploring a large volume of soil that can reach maximum values of around 5 m in depth and 30 m in horizontal extension (Moreno et al., 2005). The small decreases, observed in oaks f_c in Figure 7a during dry years, generally recovered within one or two years. This response of the tree leaf area is associated with low frequency oscillations, such as annual rainfall (Poole and Milles, 1981). This is also supported by the variance observed in f_c that can be explained by the anomalies of relative evapotranspiration of previous months. During the spring, the highest correlation coefficients are obtained for the previous two or three months (e.g. average f_c for the peak month, April, is correlated with average anomalies from February to April with an R^2 equal to 0.76 and with anomalies of the previous year with an $R^2 = 0.52$). However, during the summer, the coverage of the vegetation can be better explained by what has happened during the previous year (e.g. R^2 is equal to 0.39 for average August f_c and the anomalies of the two previous months, and 0.64 for the anomalies of the year), suggesting that those values of f_c might be linked to processes occurring at different time scales.

A more detailed analysis is required, but these results support the conclusion that the drought events characterized for this period did not cause any permanent damage to the vegetation, considering both the grasslands and the oak trees.

4 Conclusions

The SEBS model has been used to estimate monthly energy fluxes over the *dehesa* area of the Iberian Peninsula from January 2001 to August 2018. There was a satisfactory agreement between modelled fluxes and measurements obtained for three years over two sites that are representative of the ecosystem.

At both sites annual ET was very close to total precipitation, with the exception of a few wet years and those in which intense precipitation events producing a high run-off were observed. Average aridity indices for the 17 hydrological years of 2.9 and 3.75 were computed at Sta.CLo and ES_LMa, respectively, indicating that their evaporative demand cannot be met by annual precipitation of these sites, and the more arid conditions of ES_LMa.

Drought has been characterized on an annual and monthly scale over the experimental sites and the whole area of *dehesa* of the Iberian Peninsula using relative evaporation anomalies (ET/ET_o). At the annual scale, the negative anomalies of two years, 2004/2005 and 2011/2012, stood out during the study period at the experimental sites and the entire *dehesa* area. However, a recovery of average values is observed in the years following the dry ones, indicating the absence of prolonged droughts for the period. Maps of ET/ET_o anomalies showed that most of the *dehesa* area was affected in those dry years. These maps complemented the averaged data, providing spatial information about regional impacts that could be useful for a

https://doi.org/10.5194/hess-2020-190
Preprint. Discussion started: 26 May 2020
© Author(s) 2020. CC BY 4.0 License.

more detailed analysis.

On the monthly scale, the drought event of 2004/05 is confirmed as being the longest, with sixteen consecutive months of negative anomalies (from October 2004 to January 2006), and the most intense event, with peak negative values in January-February and April-May of 2005, explaining the important impact on cereal production. The dynamics of the vegetation strata on a monthly scale allows for a separate assessment of water stress impacts on oaks and pastures. The different behaviour observed in vegetation ground cover during the drier events in months with a preponderant presence of grasslands, compared with months in which only oaks were active, is consistent with the different strategies adopted by the two strata to cope with water stress. In addition, the correlation of monthly vegetation fractional coverage with previous short or medium-term anomalies (from two months to one year) suggest that those values might be linked to processes occurring on a different time scale, depending on whether the grassland or the tree is the predominant vegetation.

These results back up the conclusion that the drought events characterized for this period did not cause permanent damage to the vegetation of *dehesa* systems, considering both the grasslands and the oak trees. The approach tested has proved to be useful for providing insights into the characteristics of drought events over this ecosystem, for helping to define the issues and for identifying areas of interest for future studies at finer resolutions.

Code and data availability

SEBS code is available in GitHub repository to download (https://github.com/TSEBS/SEBS_Spain). Validation data of ES-LMa site is available at the European Fluxes Database Cluster (http://www.europe-fluxdata.eu/home/site-details?id=ES-LMa) and data of Sta.Clo site may be distributed on request to the principal investigator of Sta. Clotilde experimental site (M. P. González-Dugo, IFAPA, mariap.gonzalez.d@juntadeandalucia.es).

Acknowledgement

This work has been funded by the OECD Cooperative Research Programme: Biological Resource Management for Sustainable Agricultural Systems (contract JA00084693) and the SensDehesa (PP.PEI.IDF201601.16) project, 80% cofunded by the European Regional Development Fund, AOP 2014-2020. Additional support was provided by RTA2014-00063-C04-02 INIA-FEDER project. X.C. was supported by the National Natural Science Foundation of China (41975009), and A.A. by EU Horizon 2020 Marie Skłodowska-Curie grant agreement No. 703978. We would like to thank the owners and workers of Santa Clotilde experimental site, as well as the group managing the experimental site of Las Majadas for the eddy covariance measurements and the additional data.

https://doi.org/10.5194/hess-2020-190
Preprint. Discussion started: 26 May 2020
© Author(s) 2020. CC BY 4.0 License.

Hydrology and Earth System Sciences
Discussions

Author Contributions

M.P.G.-D. conceived the original idea, analyzed the data and took the lead in writing the manuscript; X.C. and Z.S. designed the model, the computational framework, and contributed to the interpretation of the data; M.P.G.-D. and X.C. collected the input data and performed the numerical calculations; A.A., E.C., P.G.G. and A.C. collected and analyzed the validation data and reviewed the paper. All authors provided critical feedback and helped to shape the manuscript.

References

Allen, R.G., Pereira, L.S., Raes, D., Smith, M.: Crop evapotranspiration: Guidelines for computing crop requirements. Irrigation and Drainage Paper No. 56, FAO, Rome, Italy. 1998

Allen, R.G., Irmak, A., Trezza, R., Hendrickx, J. M. H., Bastiaanssen, W., and Kjaersgaard, J.: Satellite-based ET estimation in agriculture using SEBAL and METRIC. Hydrol. Process. 25, 4011–4027, https://doi.org/10.1002/hyp.8408, 2011.

Anderson, M. C., Hain, C. R.,Wardlow, B., Pimstein, A., Mecikalski, J. R., and Kustas, W.P.: Evaluation of Drought Indices Based on Thermal Remote Sensing of Evapotranspiration over the Continental United States, J. Clim., 24-8, 2025-2044, https://doi.org/10.1175/2010JCLI3812.1, 2011.

Anderson M. C., Zolin, C. A., Hain, C. R., Semmens, K., Yilmaz, M. T., and Gao, F.: Comparison of satellite-derived LAI and precipitation anomalies over Brazil with a thermal infrared-based Evaporative Stress Index for 2003–2013. J. Hydrol. 526: 287–302 http://dx.doi.org/10.1016/j.jhydrol.2015.01.005, 2015.

Anderson, M.C., Zolin, C.A., Sentelhas, P.C., Hain, C.R., Semmens, K., Tugrul Yilmaz, M., Gao, F., Otkin, J.A., Tetrault, R.: The Evaporative Stress Index as an indicator of agricultural drought in Brazil: An assessment based on crop yield impacts. Rem. Sens. Environ. 174: 82–99. https://doi.org/10.1016/j.rse.2015.11.034. 2016.

Andreu, A., Dube, T., Nieto, H., Mudau, A.E., González-Dugo, M.P., Guzinski, R., Hülsmann, S.: Remote sensing of water use and water stress in the African savanna ecosystem at local scale – Development and validation of a monitoring tool. Phys. Chem. Earth 112, 154–164. https://doi.org/10.1016/j.pce.2019.02.004. 2019.

Andreu, A., Kustas, W.P., Polo, M. J., Carrara, A., and González-Dugo, M. P.: Modeling Surface Energy Fluxes over a Dehesa (Oak Savanna) Ecosystem Using a Thermal Based Two-Source Energy Balance Model (TSEB) I. Remote Sens., 10, 567, https://doi.org/10.3390/rs10040567, 2018.

Andreu, A., Kustas, W.P., Polo, M. J., Carrara, A., and González-Dugo, M. P.: Modeling Surface Energy Fluxes over a Dehesa (Oak Savanna) Ecosystem Using a Thermal Based Two Source Energy Balance Model (TSEB) II—Integration of Remote Sensing Medium and Low Spatial Resolution Satellite Images. Remote Sens., 10, 558, https://doi.org/10.3390/rs10040558, 2018.

Andreu, A., Timmermans, W. J., Skokovic, D., and González-Dugo, M. P.: Influence of component temperature derivation from dual angle thermal infrared observations on TSEB flux estimates over an irrigated vineyard. Acta Geophysica., doi:10.1515/acgeo-2015-0037, 2015.

Baret, F., and Guyot, G.: Potentials and limits of vegetation indices for LAI and APAR assessments, Remote Sens. Environ., 35, 161-173, 1991.

Bouchet, R. J.: Evapotranspiration reelle, evapotranspiration potentielle, et production agricole. In Annales Agronomiques (Vol. 14, pp. 743-824). 1963

Brutsaert, W., Stricker, H.: An advection-aridity approach to estimate actual regional evapotranspiration. Water Resources Research, 15(2), 443-450. 1979.

Budyko, M.I.: Climate and life, Academic Press, Orlando, FL, 1974.

Camarillo-Naranjo, J. M., Álvarez-Francoso, J. I., Limones-Rodríguez, N., Pita-López, M. F., Aguilar-Alba, M.: The Global Climate Monitor System: From Climate Data-Handling to Knowledge Dissemination. Int. J. Digital Earth, 12(4), 394-414. doi: 10.1080/17538947.2018.1429502, 2019.

https://doi.org/10.5194/hess-2020-190
Preprint. Discussion started: 26 May 2020
© Author(s) 2020. CC BY 4.0 License.

Cammalleri, C., Micale, F., and Vogt, J.: A novel soil moisture-based drought severity index (DSI) combining water deficit magnitude and frequency, Hydrol. Process., https://doi.org/10.1002/hyp.10578, 2015.

Cammalleri, C., Anderson, M.C., Ciraolo, G., D'Urso, G., Kustas, W.P., La Loggia, G., Minacapilli. M.: Applications of a remote sensing-based two-source energy balance algorithm for mapping surface fluxes without in situ air temperature observations. Remote Sens. Environ. 124 (2012) 502–515, https://doi.org/10.1016/j.rse.2012.06.009, 2012.

Carpintero E., Gonzalez-Dugo MP., Hain H., Nieto H., Gao F., Andreu A., and Kustas W.P.: Continuous evapotranspiration monitoring and water stress at watershed scale in a Mediterranean oak savanna. Proceeding SPIE 9998, Remote Sensing for Agriculture, Ecosystems, and Hydrology XVIII, 99980N, Edinburg, United Kingdom doi: 10.1117/12.2241521, 2016.

Chen, X., Su, Z., Ma, Y., Liu, S., Yu, Q., Xu, Z.: Development of a 10-year (2001-2010) 0.1° data set of land-surface energy balance for mainland China. Atmospheric Chemistry and Physics, 14(23), 13097–13117. https://doi.org/10.5194/acp-14-13097-2014, 2014.

Chen, X., Su Z., Ma Y., Middleton, E. M.: Optimization of a remote sensing energy balance method over different canopy applied at global scale, Agric. For. Meteorol. 279: 107633, https://doi.org/10.1016/j.agrformet.2019.107633, 2019.

Chen, X., Su, Z., Ma, Y., Yang, K., Wen, J., Zhang, Y.: An Improvement of Roughness Height Parameterization of the Surface Energy Balance System (SEBS) over the Tibetan Plateau. J. Appl. Meteor. Climatol. 52, 607–622. https://doi.org/10.1175/JAMC-D-12-056.1, 2013.

Choudhury, B. J., Ahmed, N. U., Idso, S. B., Reginato, R. J., and Daughtry, C. R. S.: Relations between evaporation coefficients and vegetation indices studied by model simulations. Remote Sens. Environ., 50, 1-17, 1994.

Corcobado, T., Cubera, E., Juárez, E., Moreno, G., and Solla, A.: Drought events determine performance of Quercus ilex seedlings and increase their susceptibility to *Phytophthora cinnamomi*. Agr. Forest Meteorol., 192-193, 1-8, http://dx.doi.org/10.1016/j.agrformet.2014.02.007, 2014.

Díaz, M., Campos, P. and Pulido, F. J.: The Spanish dehesas: a diversity in land-use and wildlife. In: Farming and birds in Europe: The Common Agricultural Policy and its implications for bird conservation, D. Pain y M. Pienkowski (eds.), pp. 178-209. Academic Press, London. 1997

Doorenbos, J. and Pruitt, W. O.: Crop water requirement, FAO Irrigation and Drainage, Paper N. 24, FAO, Rome, 1977.

Fenshan, R. J., and Holman, J. E.: Temporal and spatial patterns in drought-related tree dieback in Australian savanna, J. Appl. Ecol., 36, 1035-1050, 1999

Foken, T.: The energy balance closure problem: An overview. Ecol. Appl., 18, 1351–1367. doi: 10.1890/06-0922.1, 2008.

Franssen, H.J.H., Stöckli, R., Lehner, I., Rotenberg, E., and Seneviratne, S.I.: Energy balance closure of eddy-covariance data: A multisite analysis for European FLUXNET stations. Agric. For. Meteor. 150, 1553–1567, doi:10.1016/j.agrformet.2010.08.005, 2010.

García-Herrera, R., Paredes, D., Trigo, R. M., Franco-Trigo, I., Hernández, E., Barriopedro, D., and Mendes, M.: The outstanding 2004/05 drought in the Iberian Peninsula: associated atmospheric circulation. J. Hydrometeor., 8 (3), 483-498, doi: 10.1175/JHM578.1, 2007.

Gonzalez-Dugo, M.P., Neale, C.M.U., Mateos, L., Kustas, W.P., Prueger, J.H., Anderson, M.C., and Li, F.: A comparison of operational remote sensing-based models for estimating crop evapotranspiration. Agr. Forest Meteorol., 149:1843-1853, https://doi.org/10.1016/j.agrformet.2009.06.012, 2009.

González-Dugo M.P., J. González-Piqueras, I. Campos, A. Andreu, C. Balbotin, A. Calera. 2012. Evapotranspiration monitoring in vineyard using satellite-based thermal remote sensing. In: Remote Sensing for Agriculture, Ecosystems, and Hydrology XIV, C. M. U. Neale, A. Maltese (Eds.), Proc. of SPIE. Vol 8531. doi:10.1117/12.974731.

Guzinski R., Nieto, H., El-Madany, T., Migliavacca, M., and Carrara, A.:2018. Validation of Fine Resolution Land-Surface Energy Fluxes Derived with Combined Sentinel-2 and Sentinel-3 Observations. IGARSS 2018 IEEE Intl. Geosci. Rem. Sens. Symposium, Valencia, pp. 8711-8714. doi: 10.1109/IGARSS.2018.8518229, 2018.

Harris, I. P. D. J., Jones, P. D., Osborn, T. J., Lister, D. H.: Updated high-resolution grids of monthly climatic observations–the CRU TS3. 10 Dataset. Int. J. Climatol., 34(3), 623-642. doi: 10.1002/joc.3711. Revision of the paper: Revised_Appendix_3_CLD.pdf, 2014.

Hazell, P. B. R., Oram, P., Chaherli, N.: Managing droughts in the low-rainfall areas of the Middle East and North Africa.

https://doi.org/10.5194/hess-2020-190
Preprint. Discussion started: 26 May 2020
© Author(s) 2020. CC BY 4.0 License.

EPTD Discussion Paper, 78, International Food Policy Research Institute (IFPRI) pp. 45, 2001.

Jackson, R.D and Huete, A. R.: Interpreting vegetation indices. Pre. Vet. Med. ,11(3–4): 185-200, https://doi.org/10.1016/S0167-5877(05)80004-2, 1991.

Kustas W.P., and Daughtry, C.S.T.: Estimation of the soil heat flux/net radiation ratio from spectral data. Agr. Forest Meteorol., 49, 205–223, 1990.

Kustas W. P. and Norman, J. M.: Use of remote sensing for evapotranspiration monitoring over land surfaces, Hydrol. Sci. J., 41:4, 495-516 https://doi.org/10.1080/02626669609491522, 1996.

Menenti M.: Physical Aspects of and Determination of Evaporation in Deserts Applying Remote Sensing Techniques, Report 10 (special issue), Institute for Land and Water Management Research (ICW): The Netherlands, 1984.

Michel D., Jiménez, C., Miralles, D. G., Jung, M., Hirschi, M., Ershadi, A., Martens, B., McCabe, M. F., Fisher, J. B., Mu, Q., Seneviratne, S. I., Wood, E. F., and Fernández-Prieto, D.: The WACMOS-ET project – Part 1: Tower-scale evaluation of four remote-sensing-based evapotranspiration algorithms. Hydrol. Earth Syst. Sci., 20, 803–822, doi:10.5194/hess-20-803-2016, 2016.

Monteith J.L.: Principles of Environmental Physics, Edward Arnold Press., London, 1973

Moreno, G., and Pulido, F. J.: The Functioning, Management and Persistence of Dehesas, in:Agroforesty in Europe, edited by: Rigueiro-Rodróguez, A., McAdam, J., and Mosquera-Losada, M. R., Springer Link, 127-160, https://doi.org/10.1007/978-1-4020-8272-6z, 2009.

Moreno, G, Obrador, J.J., Cubera, E., Dupra, C.: Fine root distribution in Dehesas of Central-Western Spain. Plant Soil, 277:153–162, https://doi.org/10.1007/s11104-005-6805-0, 2005.

Morton, F. I.: Estimating evaporation and transpiration from climatological observations. J. Appl. Meteorol., 14(4), 488-497. 1975

Ponce, V.M., Pandey, R.P., and Ercan, S.: Characterization of drought across the climate spectrum. J. Hydrol. Eng, ASCE 5 (2), 222–224, https://doi.org/10.1061/(ASCE)1084-0699(2000)5:2(222), 2000.

Poole, D. K., Miller P. C.: The Distribution of Plant Water Stress and Vegetation Characteristics in Southern California Chaparral. The American Midland Naturalist, 105: 32-43, 1981.

Rambal, S.: The differential role of mechanisms for drought resistance in a Mediterranean evergreen shrub: a simulation approach. Plant. Cell. Environ., 16, 35–44, https://doi.org/10.1111/j.1365-3040.1993.tb00842.x, 1993.

Sánchez M. E, Caetano, P., Ferraz, J., Trapero, A.: Phytophthora disease of Quercus ilex in south-western Spain. Forest Pathol., 32, 5-18. doi:10.1046/j.1439-0329.2002.00261.x, 2002.

Schuepp, P.H., Leclerc, M.Y., MacPherson, J.I., and Desjardins, R.L.: Footprint prediction of scalar fluxes from analytical solutions of the diffusion equation. Bound.-Layer Meteorol. 50, 355–373, https://doi.org/10.1007/BF00120530, 1990.

Sheffield, J., Goteti G., Wen F., Wood, E.F.: A Simulated Soil Moisture Based Drought Analysis for the United States. Journal of Geophysical Research, 109: D24108, https://doi.org/10.1029/2004JD005182. 2004.

Sheffield, J., Wood, E.F.: Drought: Past problems and future scenarios. Earthscan London, UK, 2011.

Su Z.: The surface energy balance system (SEBS) for estimation of turbulent heat fluxes. Hydrol. Earth Sys. Sci., 6(1), 85–99, 2002.

Su Z., Yacob A., Wen J., Roerink G., He Y., Gao B., Boogaard H. and van Diepen C.: Assessing relative soil moisture with remote sensing data: theory and experimental validation. Physics Chemistry of the Earth, 28(1–3), 89–101, 2003.

UNEP: GEO Yearbook, Earthscan, London, 2006.

Vinukollu, R. K., Wood, E. F., Ferguson, C. R., and Fisher, J. B.: Global estimates of evapotranspiration for climate studies using multi-sensor remote sensing data: Evaluation of three process-based approaches, Remote Sens. Environ., 115, 801– 823, doi:10.1016/j.rse.2010.11.006, 2011.

Wardlow, B. D., Anderson, M. C., Verdin, J.P.: Remote Sensing of Drought: Innovative Monitoring Approaches. CRC Press, Taylor and Francis Group, Boca Raton, FL., 2012.

https://doi.org/10.5194/hess-2020-190
Preprint. Discussion started: 26 May 2020
© Author(s) 2020. CC BY 4.0 License.

Table 1. Input datasets used to calculate the surface energy fluxes over the Iberian Peninsula from 2000 to 2015

Variable	Data source	Spatial resolution	Temporal resolution	Method
SW_d	ERA Interim(ECMWF)*	80km	6h	Reanalysis
LW_d	ERA Interim(ECMWF)	80km	6h	Reanalysis
T_a	ERA Interim(ECMWF)	80km	6h	Reanalysis
Q	ERA Interim(ECMWF)	80km	6h	Reanalysis
u	ERA Interim(ECMWF)	80km	6h	Reanalysis
P	ERA Interim(ECMWF)	80km	6h	Reanalysis
LST	MOD11C3 V5**	0.05°	1 month	Satellite
Albedo	GlobAlbedo***/MODIS**	0.1°	1 month	Satellite
NDVI	MOD13C1 V5/MYD13C1 V5**	0.01°	16 days	Satellite

*http://apps.ecmwf.int/datasets/data/interim-land/type=fc/

**https://modis.gsfc.nasa.gov

***http://www.globalbedo.org/index.php

https://doi.org/10.5194/hess-2020-190
Preprint. Discussion started: 26 May 2020
© Author(s) 2020. CC BY 4.0 License.

Hydrology and Earth System Sciences
Discussions

Figure Captions

Figure 1: Distribution of oak savanna area in the Iberian Peninsula. Location of validation sites and pictures of eddy covariance flux towers

Figure 2. Comparison of observed and estimated monthly energy fluxes using SEBS model during three years at each oak savanna site, ES-Lma (LA) and Sta.Clo (SC).

Figure 3. Evolution of annual rainfall, ET, ETo and ET/ETo at ES-LMa site (a) and Sta.Clo site, and annual run-off at Sta.Clo watershed from 2001/02 to 2017/2018 hydrological years

Figure 4. Annual anomalies of relative evapotranspiration at the experimental sites from 2001 to 2018.

Figure 5. Annual anomalies of relative evapotranspiration for the oak savanna area of the Iberian Peninsula from 2001/02 to 2017/18

Figure 6. Spatial distribution of annual anomalies of relative evapotranspiration for the oak savanna area of the Iberian Peninsula from 2001/02 to 2017/18, the average ET/ET_o for the period and its standard deviation (STD)

Figure 7. (a) Monthly evolution of evapotranspiration anomalies (blue line), with negative values indicating drier than normal conditions (depicted in red). and green canopy cover (green line) of the oak savanna area of the Iberian Peninsula. (b) Monthly evolution of and rainfall, ET_o and ET in the same region and time interval

https://doi.org/10.5194/hess-2020-190
Preprint. Discussion started: 26 May 2020
© Author(s) 2020. CC BY 4.0 License.

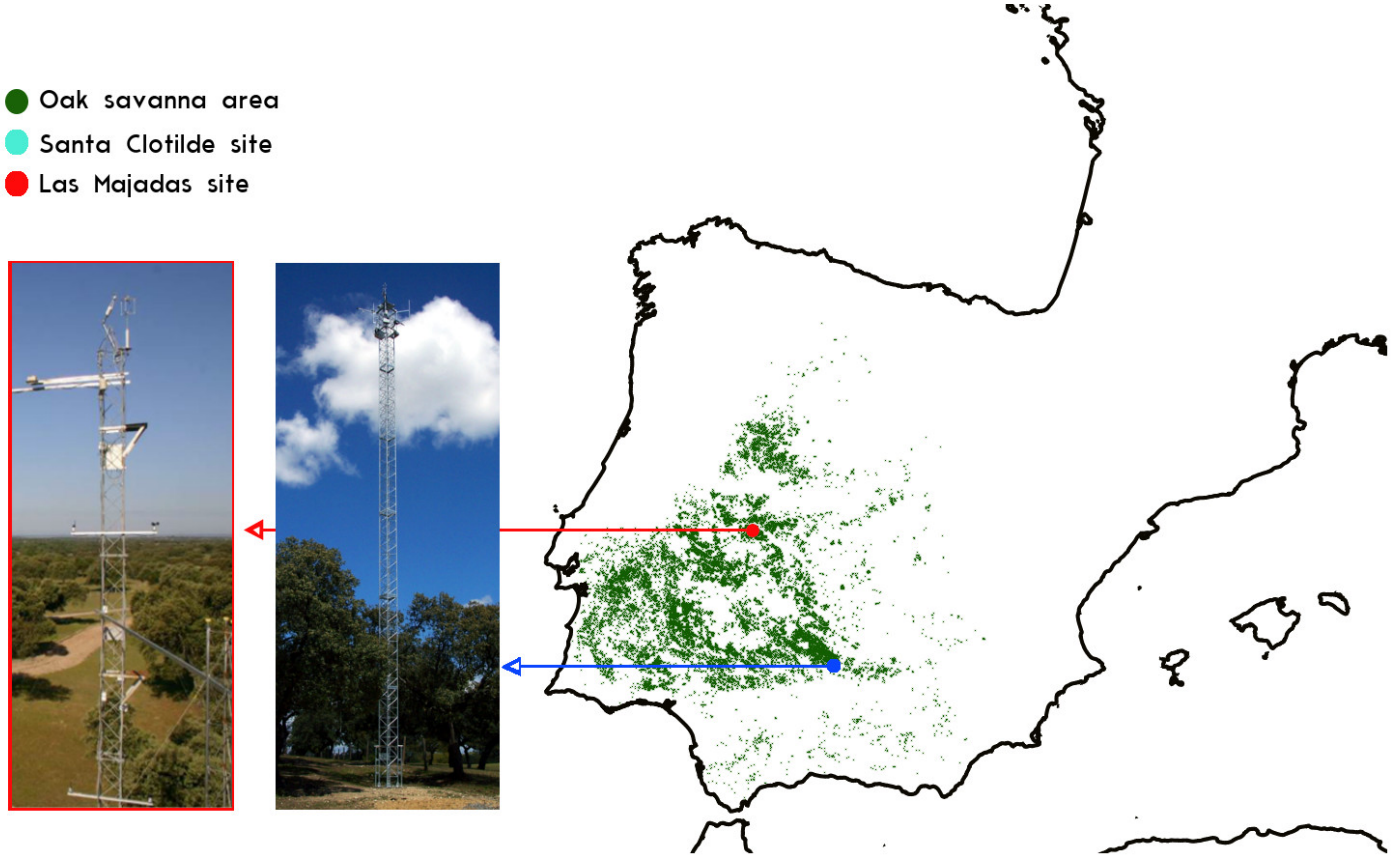

Figure 1

https://doi.org/10.5194/hess-2020-190
Preprint. Discussion started: 26 May 2020
© Author(s) 2020. CC BY 4.0 License.

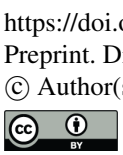

Hydrology and Earth System Sciences
Discussions

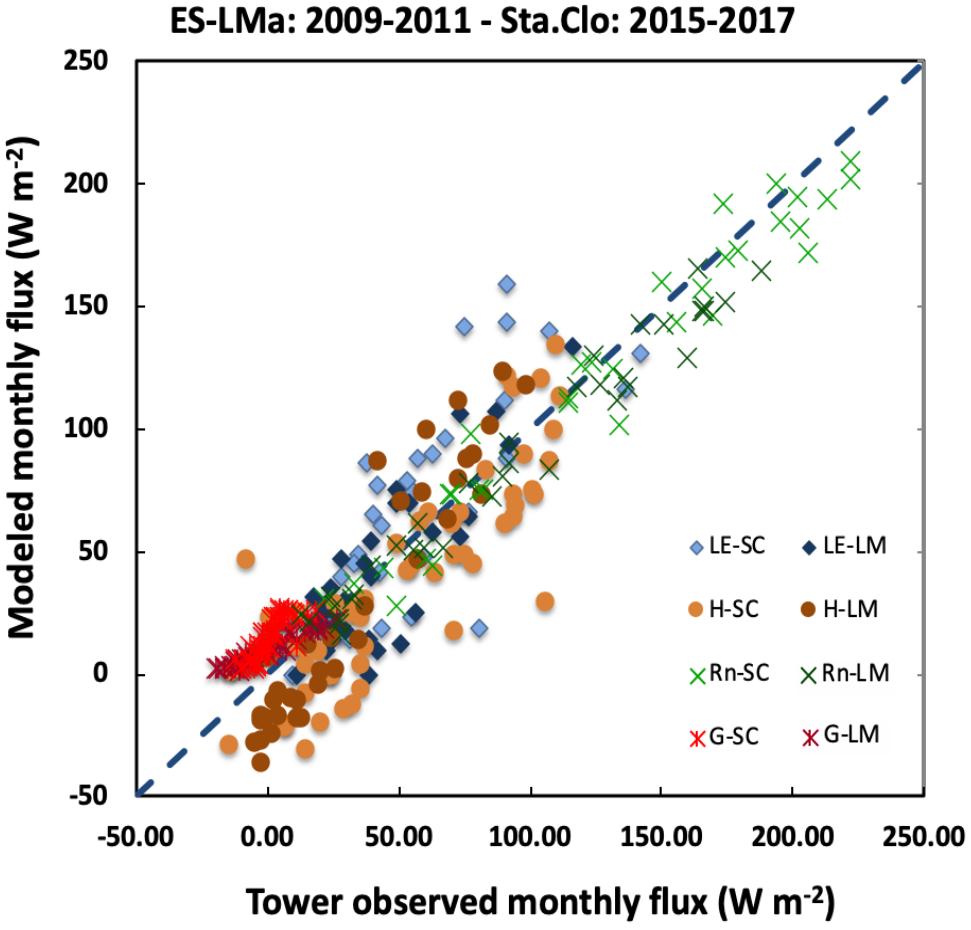

Figure 2

https://doi.org/10.5194/hess-2020-190
Preprint. Discussion started: 26 May 2020
© Author(s) 2020. CC BY 4.0 License.

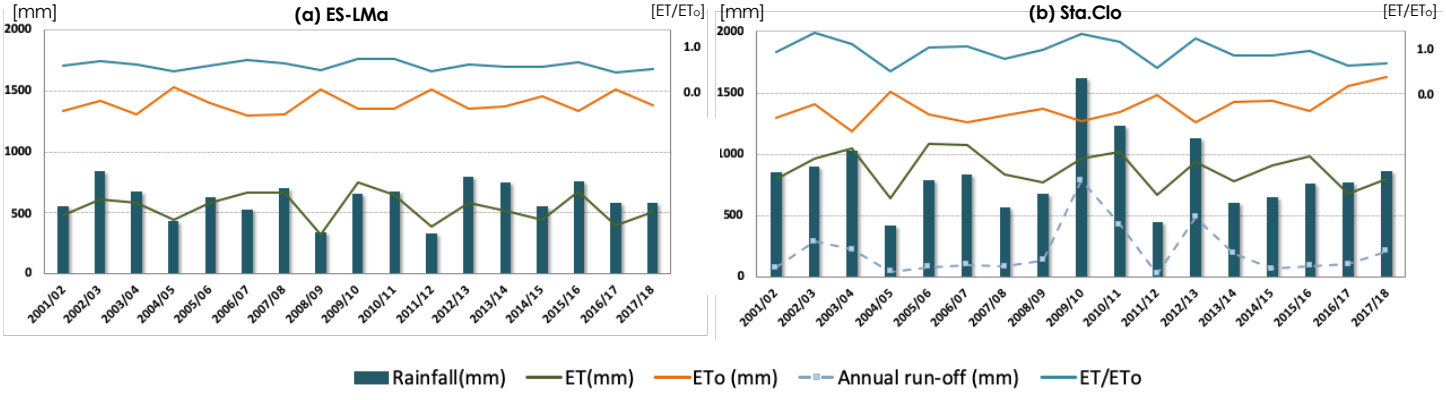

Figure 3

https://doi.org/10.5194/hess-2020-190
Preprint. Discussion started: 26 May 2020
© Author(s) 2020. CC BY 4.0 License.

Figure 4

https://doi.org/10.5194/hess-2020-190
Preprint. Discussion started: 26 May 2020
© Author(s) 2020. CC BY 4.0 License.

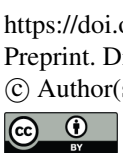

Hydrology and Earth System Sciences
Discussions
Open Access
EGU

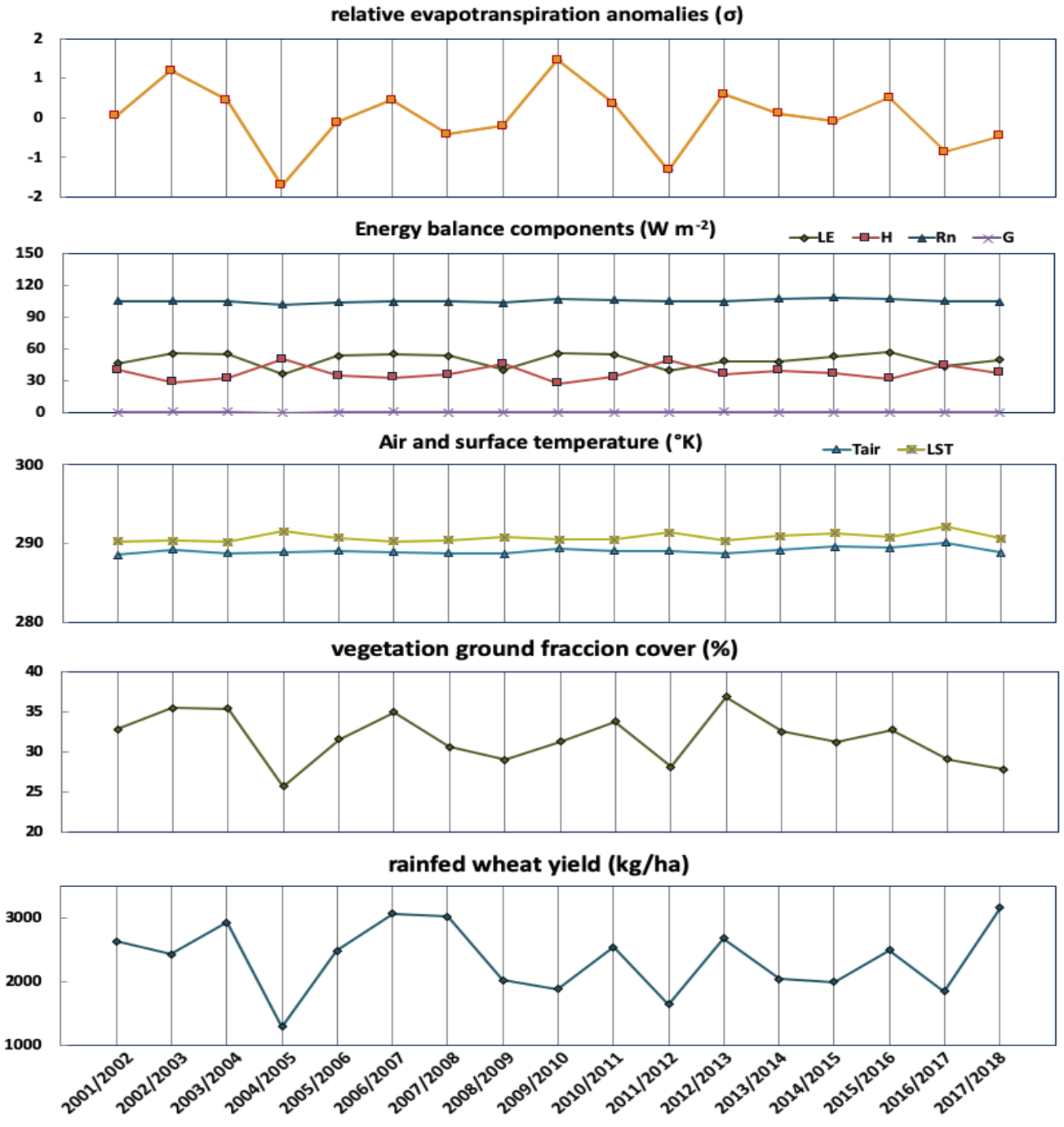

Figure 5

https://doi.org/10.5194/hess-2020-190
Preprint. Discussion started: 26 May 2020
© Author(s) 2020. CC BY 4.0 License.

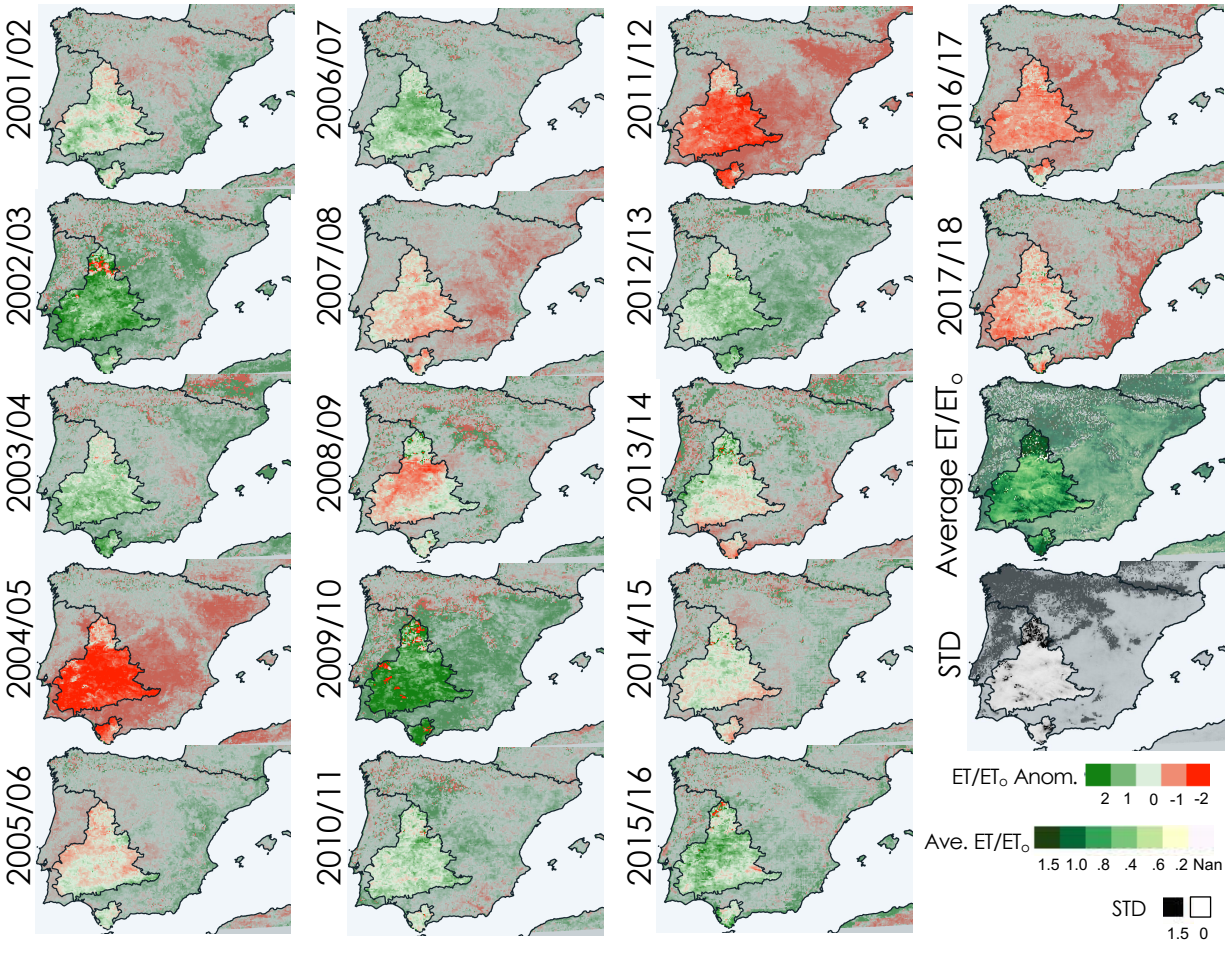

Figure 6

https://doi.org/10.5194/hess-2020-190
Preprint. Discussion started: 26 May 2020
© Author(s) 2020. CC BY 4.0 License.

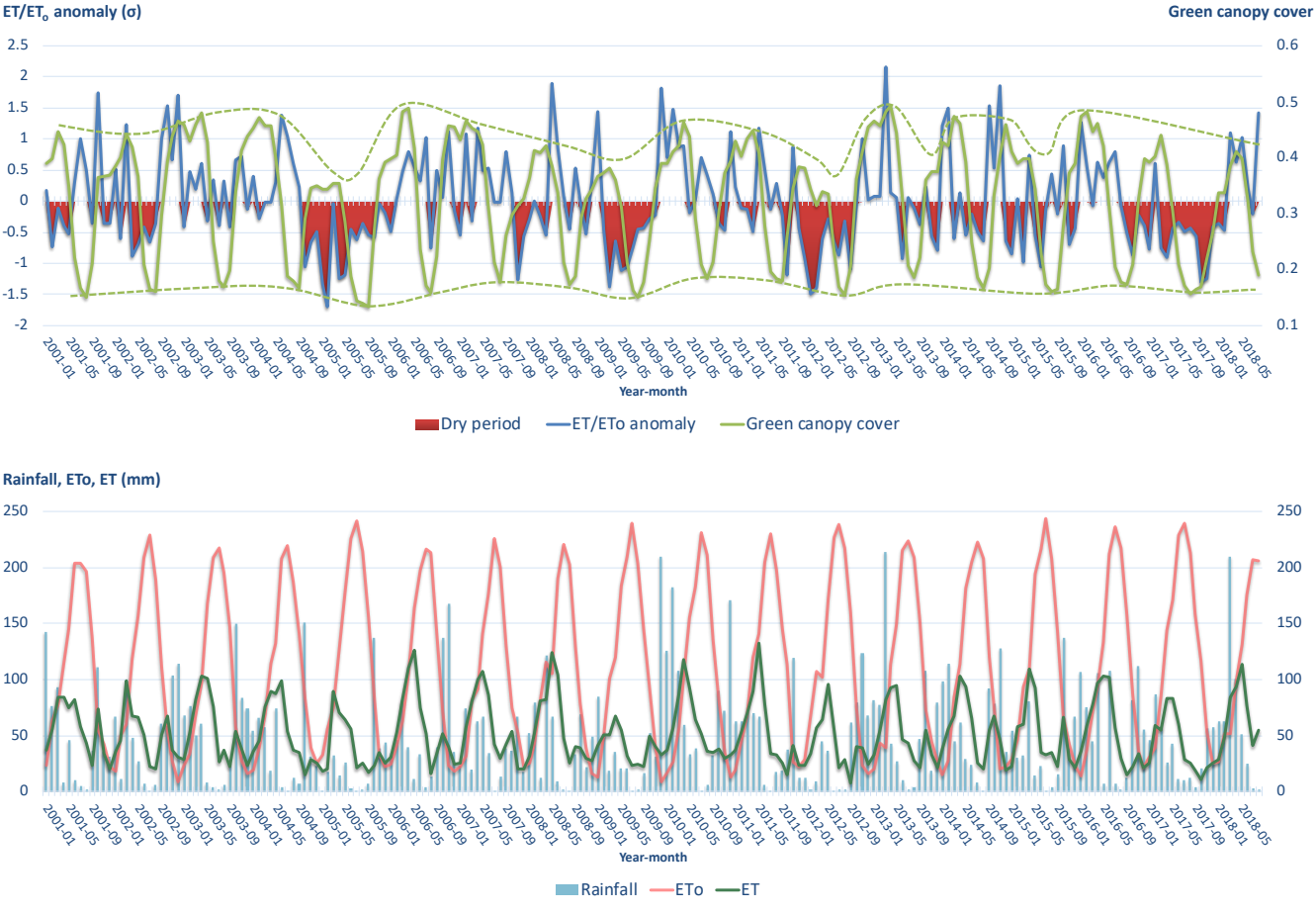

Figure 7